Journal of Energy Challenges and Mechanics
http://www.nscj.co.uk/JECM/
ISSN 2056-9386
Volume 4 (2017) issue 1, article 5

Molecular Orbital Modeling of Energy Relevant Material's Properties for Hydrogen Storage

能量相关材料储氢性能的分子轨道模型

Jerry A. Darsey

Center for Molecular Design and Development, University of Arkansas at Little Rock, Little Rock, Arkansas, 72204, USA

jadarsey@ualr.edu

Accepted for publication on 2nd January 2018

Abstract - **It is well known that the outer orbitals of an atom are responsible for their major physical and chemical properties. The computed energies of the lowest unoccupied atomic orbitals [LUAO] and the energies of the highest occupied atomic orbitals [HOAO], which were obtained using an *ab initio* molecular orbital program. These orbital energies were correlated with the properties, both physical and chemical, of the bulk materials made from these various atomic systems using artificial neural network (ANNs) modeling procedures. This paper will present results of the modeling studies of single atoms and small atomic clusters for elements beginning with potassium through selenium and rubidium through tellurium. This paper will present results that show several chemical and physical properties of the bulk material properties of materials are modeled by our computational procedures. The clusters were initially modeled using *HyperChem 5.01* molecular modeling software. This program was used to construct and optimize the various atomic clusters. Spin multiplicity for the lowest ground state as determined from term symbols were used also for geometry optimizations on these atomic clusters. *Guassian 03* molecular modeling software was then used to perform density functional theory (DFT) single point energy calculations on the structurally optimized atoms. In the *Guassian (03)* program, the LanL2DZ basis set and the B3PW91 functional was used. The LanL2DZ basis set incorporates parameters that accounts for the relativistic effects of heavier elements. In addition, materials used for the storage of hydrogen gas were also modeled and will be discussed in this talk.**

Keywords - **molecular orbital modeling, energy relavent material's properties, *ab initio* molecular orbital, Density Functional Theory, Artificial Intelligence, Artificial Neural Networks, hydrogen storage, Metal-Organic Frameworks.**

I. Introduction

Artificial Intelligence (AI) is becoming a more and more used procedure in many areas of science. In the July 7, 2017 issue of *Science*, many applications of AI are highlighted [1]. For example, recent developments in using artificial neural networks (a type of artificial intelligence) is used by organic chemists to understand and predict the outcome of organic chemical reactions [2]. Another example is where plant biologist use AI to predict protein-protein interactions in order to find out how proteins interact [3].

An artificial neural network (ANN) is a parallel distributed processing system. In a multi-layer network, the information is propagated from the input layer (experimental data), to the hidden layer, to the output layer (parameters to be predicted), in a manner that the relationship between input and output is generally nonlinear. This property of a multi-layer

network lends itself to efficient interpolation and estimation of a set of parameters from experimental measurements [4,5].

In a feed forward network, the processing elements (PEs) are interconnected through unidirectional information channels. The key to the success of developing an artificial neural network to model this relationship is to train the network with as many examples as reasonable in order to capture the essence of the data. See Figure 1 for an example of the architecture of a typical artificial neural network.

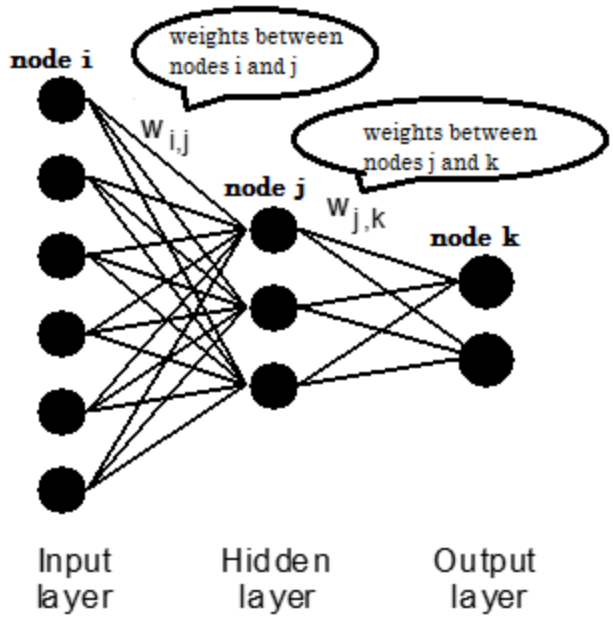

Figure 1 Architecture of typical artificial neural network

Note that the key to the success of an artificial neural network is to have as many training examples as possible. An ANN needs to have sufficient nodes in the hidden layer to allow for the network to make generalizations in correlations between the input data and the output data. If there are too many nodes, the network will "memorize" rather than generalize [6-8]. This unique property of neural networks has been exploited in this work. Neural network models are specified fundamentally by architectures, transfer functions and learning laws [6, 8]. In this work, the trained network of 70 different organic compounds on which the corresponding physical properties of boiling point (B.P.), melting point (M.P.), refractive indes (R.I.), density (D), and dipole moment (D.M.) were provided and then asked our "trained" neural network to perdict the molecular weight. The predicted four compounds at a time, that is if one took out four compounds from the training set and then trained on the remaining 66 coumpounds. Next the four compounds removed were propagated and predicted for their molecular weights. This was repeated about 20 times, always removing four compounds and training on the 66 remaining, until all compounds had its turn of being removed from training and were propagated. The results of this can be seen in Figure 2 in the Results section of this manuscript.

II. Methods I: Prediction of molecular weights

In the training part of this project, a standard three layer network architecture as seen in Figure 1. The artificial neural network was a typical feed-forward, back-propagation newwork using software developed by NASA [9] but modified by our group for our purposes. Our input layer consisted of five nodes, one for each physical property being trained on. Our second layer (hidden layer), consisted of 28 nodes and our output layer was a single node representing molecular weights. Our network was completely interconnected; that is every node was connected to every other node (See Figure 1).

One final point needs to be pointed out. In preparing the input data, is is necessary to normalize all the physical property values to numbers between 0.1 and 0.9. The is necessary because of the transfer function, which is a sigmoid activation function that is asymptopic between 0.0 and 1.0 [9]. The mathamatical form of the equation is

$$\boldsymbol{f(x) = 1(1 + e^{-(x+T)})^{-1}} \quad (1)$$

where T is a simple threshold, x is the input value and f(x) is the normalized number. For simplification, the threshold was set to zero.

Methods II: Prediction of Metal Hydrides' Hydrogen Storage.

Metal hydrides are a class of materials that are being researched for its potential for storing hydrogen [10-12]. Metal hydrides are a safe fuel-adsorbing candidate that would keep the hydrogen bound to a metal until it is needed to provide fuel during vehicle operation [11]. Metal hydrides store hydrogen much more compactly than using pressurized hydrogen, or liquid hydrogen. In addition, if the container itself were damaged there would not be a catastrophic fuel release [13,14]. Several hydrides are potential lightweight candidates for future materials, especially those with dopants [15,16]. Other metals are being investigated for other properties that have advantages in solar energy or as parts of a fuel cell. Cyclability and kinetics are improved by adding dopants to metal hydrides. It is hoped that a computational method can produce several material candidates for hydrogen storage and evaluate their viability and efficiency as a metal hydride. This study is focused on several excellent metals capable of adsorbing hydrogen. A well-studied group was selected from a section of the metal hydride database [17]. The properties that were focused on are well-established criteria that improve the performance of metal hydrides. The range of properties is wide enough for a large distribution in the predictability. The main elements of the study use density functional theory (DFT) using the Gaussian 03 quantum mechanical software [18] and artificial neural network modeling. Some of the bulk properties predicted were melting point, boiling point, first ionization energy, dipole moment and hydrogen adsorption. The highest occupied molecular orbitals (HOMOs) and lowest unoccupied molecular orbitals (LUMOs) were used as inputs for the artificial neural network and the bulk physical properties were used in the output.

III. Results—Molecular weight predictions

Our artificial neural network was trained on 66 compounds and tested the results of the training on four molecules. The compounds used for training and testing along with the five physical properties listed in Table I. The five physical properties are boiling point (B.P.), melting point (M.P.), refractive indes (R.I.), density (D), and dipole moment (D.M.). These properties were found in the 87th addition of the *CRC Hanbook of Chemistry and Physics* [19]. The molecules used for training and testing purposes were varied. Table 3 of Appendix II shows the molecular weiths for the 70 molecules used for training and testing purposes. Performing the procedure for testing the accuracy of our artificial neural network in predicting the molecular weights of the 70 molecules results can be found in Table 2 of Appendix I.

Four molecules were randomly removed from the total of 70 molecule set and trained on the remaining 66 molecules. For example, our first

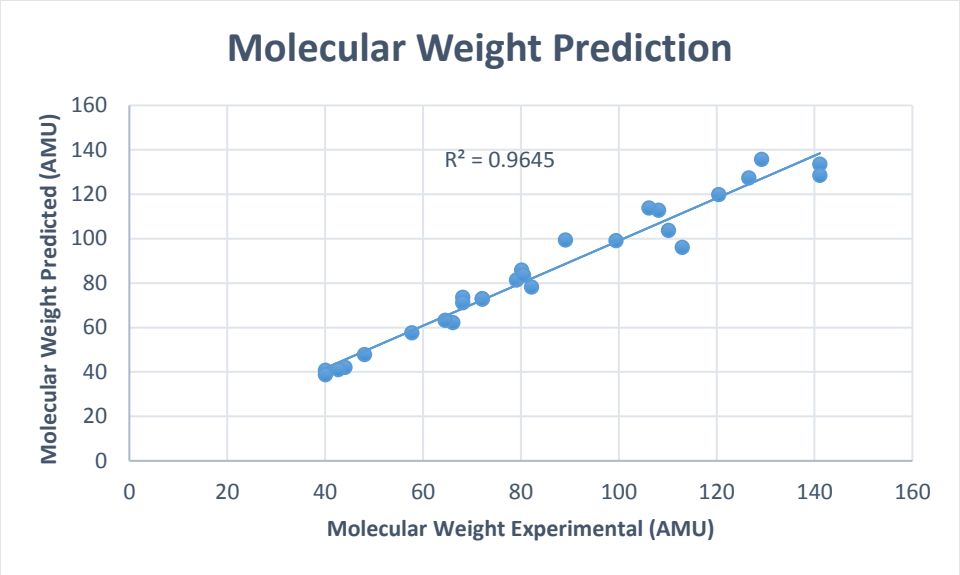

Figure 2 Molecular weight predictions using artificial neural network

training (Run 1) was performed on molecules 1 through 14, 16 through 23, 25 through 47, 49 through 63, and 65 through 70. The first molecules tested were on the training on molecules 15, 24, 48, and 64. The percent error ranged from 1.35% to 5.71% with an average error in the prediction of the molecular weights for Run 1 at 3.21%. Run 2, the neural network was trained on molecules 1 through 12, 14 through 27, 29 through 55, and 57 through 69. Next there was testing on molecules 13, 28, 56, and 70. In this training, the percent error ranged from 0.55% to 7.00% with an average error in predicting the molecular weights of the four tested molecules at 3.61%. This procedure was repeated for 26 total runs. In these runs, every molecule was included at least once in a testing set. The overall average error for all 26 runs was 3.11%. When a constructed correlation plot of experimental molecular weight vs. neural network predicted molecular weights (Figure 2), an obtained R^2 of 0.9645 was obtained. This is consider a very accurate correlation.

One point of importance is that numerous runs were made in which the elimination of one of the physical properties from the training set. In all cases, the network was unable to make accurate predictions of the molecular weights. It was found that it required all five physical properties in the training set in order to get accurate predictions of the molecule weights.

Another point to be made is that when several additional trainings were made with the removal of one of the five physical properties and substituted with the molecular weight for that property with the network was trained on the set on the four physical properties remaining, it was found that the network trained to the removed property but with much more overall average error. The average error was usually in excess of 20 percent. It is unsure why it did not train as well on the physical properties when the molecular weight became one of the training parameters.

IV. Results—Metal hydride predictions

The results of the calculations on various metal hydride clusters are shown in Figure 3 and summarized in Table 1 [20]. It can be seen that the wt. percnet hydrogen gas adsorbed ranged from a high of 7.66% to a low of 0.72%. The correlation plot shown in Figure 3 is for a fully cross validated training. That is, each cluster was allowed to be excluded from the input data for the neural network, where the remaining 10 clusters were in the training set. Each metal hydride cluster had its turn being predicted. When a plot of the neural network predicted values for wt. % hydrogen adsorbes vs. experimental wt. hydrogen adsorbed, the correlation had an R^2 value of 0.9569. This is a very good correlation considering the error associated with these experimental results.

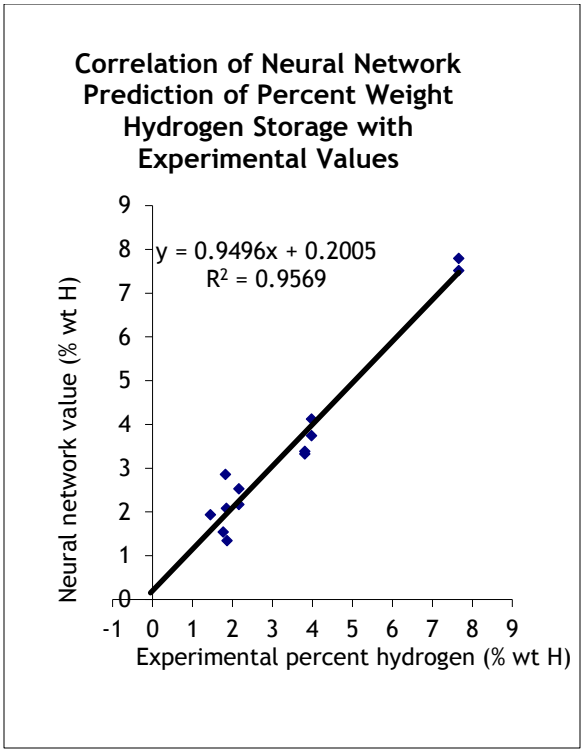

Figure 3 Percent wt. hydrogen adsorbed predictions using artificial neural network modeling.

Table 1: Metals and experimental data used in Figure 3.

Metal	**Pressure (atm) at 25 °C**	**Temperature for one atmosphere of pressure ºC**	**Weight percent hydrogen**
Zr	6.4×10^{-28}	881	2.16%
V	2.1	12	3.81%
Ti	4E-20	643	3.98%
Pd	0.0082	147	0.72%
Mg	0.000001	279	7.66%
TiFe	4.1	-8	1.86%
Mg_2Ni	0.00001	255	3.6%
ZrNi	0.0000004	292	1.85%
$ZrMn_2$	0.001	167	1.77%
$ZrCr_2$	0.0029	166	1.82%
TiCo	0.004	135	1.45%

V Hydrogen adsorption upon the magnesium surface

Until recently, the only pathway for H_2 adsorption onto conventional magnesium thin films was the [001] surface. With the discovery of Mg nanoblade/nanotree fabrication, there are now multiple surfaces for adsorption. A keen understanding of each surface's hydrogen adsorption kinetics is a key part of deciding if these surfaces present a more attractive hydrogen storage material than conventional thin films [21]. This study focused on the use of *ab-initio* methods to compare the adsorption of H_2 molecules onto the [001], [100], and [110] surfaces as well as an analysis of hybrid functionals and their advantages over traditional functionals for minimum energy pathway calculations. Now in building the Mg surfaces Gaussview was chosen as the primary method for constructing the surfaces. The surfaces were modeled with six layers and a 3x3 Mg surface. The resulting 54 atom structure was allowed to relax with a 10 Å vacuum space above the surface. Of the initial six surfaces proposed for study, only four were able to be stabilized. These four surfaces were manipulated via Gaussview software as part of the Gaussian 03 program, to create the initial state (IS) and the final state (FS). For the IS, a H_2 molecule was placed in the center and 5Å from the surface. For the FS, two H atoms were placed on the surface over the hcp and fcc holes. The [001] Mg IS and FS are shown in Figure 4.

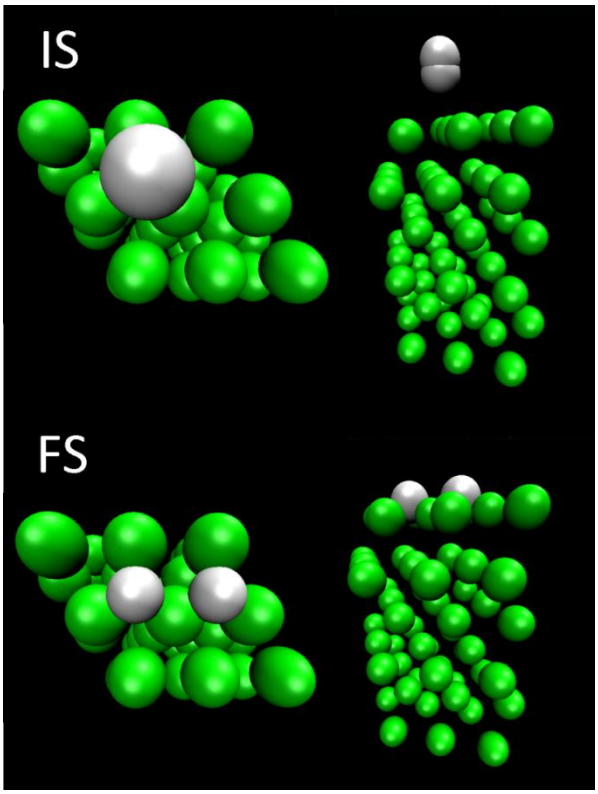

Figure4. Initial State (IS) and Final State (FS) for H_2 and the Mg [001] surface.

Overall, it was found that the [100] surface does appear to have a 20-30% lower energy of activation than the [001]. This is significant enough to encourage further runs, which could provide more accurate and insightful information as to why this is the case. The relationship of the adsorption energies of the [100] as compared to the [001] surface is difficult to ascertain. Without physisorption, the H_2 adsorption is slowed by the large activation energy required to break the H_2 bond thus backing the experimental literature claims of the high temperature, pressures, and times required for H_2 adsorption on pure Mg surfaces. The effects of the surface structure reduced the activation energy (E_a) values of the H-Mg adsorption process by 20-30% in the case of the [100] surface, while it appeared to increase the E_a values in the case of the [110] surface by 10% or more. The differences in calculated activation and adsorption energy for the [100] and [110] surfaces highlight the potential impact that the non-close packed Mg planes could have upon the adsorption kinetics of H_2 [22,23]. However, it is clear that without the capability to conduct H_2 physisorption, pure magnesium will never provide the kinetics exhibited by Mg surfaces doped with transition state metals. When combined with very small dopant percentages, the improved kinetics exhibited by the [100] surface could, however, provide the small boost necessary for hydrogen to rapidly adsorb and desorb from the surface at lower temperatures and pressures.

VI Summary

In summary it was found that an artificial neural network could successfully make an association between the five bulk physical properties, melting point, boiling point, density, refractive index and dipole moment with the molecular weight of the various organic molecules. It was also noted that it was not able to make this correlationwhen one or more of these properties was eliminated from the training set. This seems to imply that there is a functional relaton between all of these physical propertiesand molecular weight. It is also believed that there is probably hidden within these properties geometrical information about these molecules. Future studies whould be able to shed light on this possibility.

There is also the possibility of analyzing the weight space of the network $w_{i,j}$ and $w_{j,k}$, (see Figure 1). It is hypothesized that there probably exist a mathamatical relationship between the five physical properties and the molecular weights. If there were the ability to find such a relationship, one could solve for any of these properties or solve for the molecular weight as long as all of the properties and molecular weights are known for a particular molecule.

For additional information on artificial neural networks and the theory of neural networks, see references 24-30 and references therein [24-30].

This research also shows that non-close packed planes present a legitimate case for further research, either as pure magnesium surfaces or with very low dopant levels, towards the goal of discovering a plausible solution to the DOE hydrogen storage challenge. For additional information on Mg surface studies and its use in hydrogen storage, see references 21 to 23 and references within [21-23].

References

[1] Jeremy Berg, Ed. *Science*, "AI Transforms Science", **357,** pp. 16-30, 2017.

[2] Robert F. Service, *Science*, "Neural Networks learn the art of chemical synthesis", **357,** p. 27, 2017.

[3] Jennifer Sills, *Science*, "Artificial Intelligence in research", **357,** pp. 28-30, 2017.

[4] J. A. Darsey, D. W. Noid, B.R. Upadhyaya, *Chem. Phys. Lett*., "Application of neural network computing to the solution for the ground-state eigenenergy of two-dimensional harmonic oscillators", **177,** pp. 189-194, 1991.

[5] J.A. Darsey, A. G. Soman, *Makromol. Chem. Theory and Simul*., "Artificial neural system modeling of Monte Carlo simulations of polymers", **2,** pp. 711-719, 1993.

[6] M. Caudell, *A. I. Expert*, "Neural Network Primer, Part I", pp. 46-52, 1987.

[7]] M. Caudell, *A. I. Expert*, "Neural Network Primer, Part II", pp. 55-61, 1988.

[8] R. P. Lippman, *IEEE ASSP Magazine*, "An Introduction to Computing with Neural Nets", **42,** pp. 422, 1987.

[9] P.T. Baffer, *NNETS* Program, version 2.0, Johnson Space Report No. 23366, NASA, September, 1989.

[10] B. Sakintuna, F. Lamari-Darkrim, M. Hirscher, *Int J Hydrogen Energy*, "Metal hydride materials for solid hydrogen storage: A Review", Volume 32, Issue 9, pp 1121-1140, 2007.

[11] P Jena, "Materials for Hydrogen Storage: Past, Present, and Future", *J. Phys. Chem. Lett.*, ***2*** (3), pp 206–211, 2011.

[12] E. Kikkinides, M. Georgiadis, A. Stubos, "On the optimization of hydrogen storage in metal hydride beds*", J. Hydrogen Energy*, **31**, pp. 737-751, 2006.

[13] B. D. MacDonald and A. M. Rowe, *J. Power Sourc.* 174, 1, pp 282-293., 2007.

[14] E. Varkaraki, N. Lymberopoulos, E. Zoulias, D. Guichardot, and G. Poli, *Int. J. Hydrogen Energ. 32*, 10-11, pp 1589-1596, 2007.

[15] B. Bogdanovic and M. Schwickardi, J. Alloys Compd. 253-254, pp. 1-9, 1997

[16] H. Gunaydin, K.N. Houk, V. Ozolins, Proc. Natl. Acad. Sci.U.S.A., 105, 10, pp. 3673-3677, 2008.

[17] Sandia National Labs Hydride Properties Database; Sandia National Labs, U.S. Department of Energy Program, Livermore, CA, (accessed May, 2005)

[18] *Gaussian 03*, Revision E.05, Frisch, M. J.; Trucks, G. W.; Schlegel, H. B.; Scuseria, G. E.; Robb, M. A.; Cheeseman, J. R.; Montgomery, Jr., J. A.; Vreven, T.; Kudin, K. N.; Burant, J. C.; Millam, J. M.; Iyengar, S. S.; Tomasi, J.; Barone, V.; Mennucci, B.; Cossi, M.; Scalmani, G.; Rega, N.; Petersson, G. A.; Nakatsuji, H.; Hada, M.; Ehara, M.; Toyota, K.; Fukuda, R.; Hasegawa, J.; Ishida, M.; Nakajima, T.; Honda, Y.; Kitao, O.; Nakai, H.; Klene, M.; Li, X.; Knox, J. E.; Hratchian, H. P.; Cross, J. B.; Bakken, V.; Adamo, C.; Jaramillo, J.; Gomperts, R.; Stratmann, R. E.; Yazyev, O.; Austin, A. J.; Cammi, R.; Pomelli, C.; Ochterski, J. W.; Ayala, P. Y.; Morokuma, K.; Voth, G. A.; Salvador, P.; Dannenberg, J. J.; Zakrzewski, V. G.; Dapprich, S.; Daniels, A. D.; Strain, M. C.; Farkas, O.; Malick, D. K.; Rabuck, A. D.; Raghavachari, K.; Foresman, J. B.; Ortiz, J. V.; Cui, Q.; Baboul, A. G.; Clifford, S.; Cioslowski, J.; Stefanov, B. B.; Liu, G.; Liashenko, A.; Piskorz, P.; Komaromi, I.; Martin, R. L.; Fox, D. J.; Keith, T.; Al-Laham, M. A.; Peng, C. Y.; Nanayakkara, A.; Challacombe, M.; Gill, P. M. W.; Johnson, B.; Chen, W.; Wong, M. W.; Gonzalez, C.; and Pople, J. A.; Gaussian, Inc., Wallingford CT, 2004.

[19] *CRC Handbook of Chemistry and Physics*, David R. Lide, editor, 87th edition, 2006.

[20] W. Griffin and J. Darsey. "Bulk Metallic System Modeling of Metal Hydride Dimer and Trimer Nanoclusters". Journal of Computational and Theoretical Nanoscience, **7**, 1114-1119, 2010.

[21] M. Cansizoglu, F. Watanabe, P. Wang, T. Karabacak, In *Evolution of crystal orientation in obliquely deposited magnesium nanostructures for hydrogen storage applications*, 2007.

[22] T. Karabacak, G. Wang,. T. Lu, "Quasi-periodic nanostructures grown by oblique angle deposition". *J. Appl. Phys., 94*, 7723-7728, 2003

[23] M. Cansizoglu, T. Karabacak,, In *Enhanced Hydrogen Storage Properties of Magnesium Nanotrees by Glancing Angle Deposition;* **56**, 2011.

[24] P.D. Wasserman, *Neural Computing Theory and Practice*, Van Nostrand Reinhold, New Youk, 1992.

[25] J. M. Zurada, *Introduction to Artificial Neural Systems*, Weit Publishing Company, New York, 1992.

[26] H. Cartwright, editor, *Artificial Neural Networks*, Springer Science, New York, 2015.

[27] C. Dagli, A. Buczak, D. Enke, M. Embrechts, O. Ersoy, editors, *Intelligent Engineering Systems Through Artificial Neural Networks*, vol *17*, ASME Press, New York, 2007.

[28] W. Griffin, J. Darsey, Bulk Metallic System Modeling of Metal Hydride Dimer and Trimer Nanoclusters. *J. Comput. Theor. Nanosci.* **7**, 1114-1119, 201*0*

[29] W. Griffin, J. Darsey, "Artificial neural network prediction of metal hydride properties with experimental and/or computational data", *Abstr. Pap. Am. Chem. Soc.* ***235***, 132-COMP, 2008.

[30] W. Griffin, J. Darsey, COMP 314, "Molecular symmetry and variational perturbation theory in analytic density functional theory". *Abstr. Pap. Am. Chem. Soc., 233*, 232-COMP, 2007.

Appendix I

Table 2. Organic compounds and their five physical properties: melting point (M.P.), boiling point (B.P.), density (D), refractive index (R.I.) and dipole moment (D.M.).

No.	Compound Name	M.P. ^{o}C	B.P. ^{o}C	D g/cc	R.I.	D.M. debyes
1.	Dichlorofluoro methane	-135.0	9.0	1.405	1.3724	1.29
2.	Dibromo methane	-52.55	97.0	2.4970	1.5420	1.43
3.	Nitro methane	-28.50	100.8	1.1371	1.3817	3.46
4.	Pentachloro ethylene	-29.00	162.0	1.6796	1.5025	0.92
5.	Chloro ethylene	-153.8	-13.4	0.9106	1.3700	1.45
6.	Ethanal	-121.0	20.80	0.78	1.3316	2.69
7.	Chloro ethane	-136.4	12.27	0.8978	1.3576	2.05
8.	Fluoro ehtane	-143.2	-37.7	0.0022	1.2656	1.94
9.	Iodo ethane	-108.0	72.30	1.9358	1.5133	1.91
10.	Acetylamine	82.30	221.2	0.99	1.4278	3.76
11.	Dimethyl sulphoxide	18.45	189.0	1.1014	1.4770	3.96
12.	Dimethyl amine	-93.00	7.40	0.680	1.3500	1.03
13.	Propyne	-101.5	-23.2	0.70	1.386	0.78
14.	2-chloro propene	-137.4	22.65	0.9017	1.3973	1.66
15.	Propene	-185.2	-47.4	0.5193	1.357	0.37
16.	2,2-dichloropropane	-33.80	69.30	1.1120	1.4148	2.27
17.	1-propanol	-126.5	97.40	0.8035	1.3850	1.68
18.	Trimethyl amine	-117.2	2.87	0.671	1.3631	0.61
19.	Furan	-85.65	31.36	0.9514	1.4214	0.66
20.	Thiophene	-38.25	84.16	1.0649	1.5289	0.55
21.	1,2 butadiene	-136.2	10.85	0.676	1.421	0.40
22.	Butanal	-99.00	75.70	0.8170	1.3843	2.72
23.	Cyclopentene	-135.1	44.24	0.7720	1.4225	0.20
24.	Pyridine	-42.00	115.5	0.9819	1.5095	2.19
25.	Bromobenzene	-30.82	156.0	1.4950	1.5597	1.70
26.	Nitrobenzene	5.7	210.8	1.2037	1.5562	4.22
27.	Phenol	43.0	70.86	1.0576	1.5418	1.45
28.	p-chloro toulene	7.5	162.0	1.0697	1.5150	2.21
29.	Toulene	-95.0	110.6	0.8669	1.4961	0.36
30.	o-xylene	--25.18	144.4	0.8802	1.5055	0.62
31.	Dibutyl ether	-95.30	142.0	0.7689	1.3992	1.17
32.	Quinoline	-15.60	238.1	1.0929	1.6268	2.29
33.	Isoquinoline	26.50	243.3	1.0986	1.6148	2.73
34.	Phenylbenzene	71.00	255.9	0.8660	1.5880	0.00
35.	Tribromo methane	8.30	149.5	2.8899	1.5976	0.99
36.	Iodo methane	-66.45	42.40	2.2790	1.5382	1.62
37.	Ethanethiol	-144.4	35.00	0.8391	1.4310	1.58

38.	Propanone	-95.35	56.20	0.7899	1.3588	2.88
39.	Butane	-138.4	-0.50	0.601	1.354	< 0.05
40.	Dipropyl ether	-122.0	91.00	0.7360	1.3809	1.21
41.	Fluoro methane	-141.8	-78.4	0.80	1.1727	1.85
42.	1,1-dichloro ethane	-16.98	57.28	1.1757	1.4164	2.06
43.	1,1-difluroethane	-117.0	-24.7	0.9500	1.3010	2.07
44.	2-propanol	-89.50	82.40	0.7855	1.3776	1.66
45.	1-nitropropane	-108.0	130.5	1.01	1.4016	3.66
46.	2-chloropropane	-117.2	35.74	0.8617	1.3777	2.17
47.	Aniline	-6.30	184.1	1.0217	1.5863	1.53
48.	Butanal	-99.0	75.7	0.8170	1.3843	2.72
49.	m-dichloro-benzene	-24.7	173.0	1.2884	1.5459	1.72
50.	m-fluoro-toulene	-87.7	116.0	0.9986	1.4691	1.86
51.	Ethane	-183.3	-88.6	0.5720	1.0377	0.00
52.	Propadiene	-136.0	-34.5	1.7870	1.4168	0.00
53.	Propene	-185.3	-47.4	0.5193	1.357	0.37
54.	Acetylene	-80.8	-84.0	0.60	1.0005	0.00
55.	2-chloro-ethanol	-67.5	128.0	1.2002	1.4419	1.78
56.	1,3 chclohexadiene	-89.0	80.50	0.8405	1.4755	0.44
57.	1-Hexyne	-131.9	71.30	0.7155	1.3989	0.83
58.	1,4-dichloro-butane	-37.3	153.9	1.1408	1.4542	2.22
59.	Ethanoic acid	16.6	117.9	1.0492	1.3716	1.74
60.	1,3-dichloro propane	-99.5	120.4	1.1878	1.4487	2.1
61.	2-chloro-2-methyl propane	-25.40	52.0	0.8420	1.3857	2.13
62.	m-chloro-nitro benzene	24.0	235.0	1.34	1.5374	3.73
63.	p-chloro-nitro benzene	83.6	242.0	1.3	1.538	2.83
64.	1,3-cyclopentadiene	-97.2	40.00	0.8021	1.4440	0.42
65.	1,3-butadiene	-108.91	-4.41	0.6211	1.429	0.00
66.	4-chloro-phenol	43.20	219.8	1.27	1.5579	2.11
67	1,3-cyclohexadiene	-89.0	80.5	0.8405	1.4755	0.44
68.	Phenyl-methanol	-15.3	205.3	1.0419	1.5372	3.02
69.	Acetophenone	20.5	202.0	1.0281	1.5372	3.02
70.	p-fluoro-nitrobenzene	27.0	206.0	1.3300	1.5316	2.87

Appendix II

Table 3. Molecular weights of molecules with physical properties given in Table I.

No.	Compound Name	Molecular Weight (AMU)
1.	Dichlorofluoro methane	102.92
2.	Dibromo methane	173.85
3.	Nitro methane	61.04
4.	Pentachloro ethylene	202.30
5.	Chloro ethylene	62.5
6.	Ethanal	44.05
7.	Chloro ethane	64.52
8.	Fluoro ehtane	48.06
9.	Iodo ethane	155.97
10.	Acetylamine	59.07
11.	Dimethyl sulphoxide	78.13
12.	Dimethyl amine	45.09
13.	Propyne	40.07
14.	2-chloro propene	76.53
15.	Propene	42.08
16.	2,2-dichloropropane	112.99
17.	1-propanol	60.11
18.	Trimethyl amine	59.11
19.	Furan	68.08
20.	Thiophene	84.14
21.	1,2 butadiene	54.09
22.	Butanal	72.12
23.	Cyclopentene	68.13
24.	Pyridine	79.10
25.	Bromobenzene	157.02
26.	Nitrobenzene	123.11
27.	Phenol	94.11
28.	p-chloro toulene	126.59
29.	Toulene	92.15
30.	o-xylene	106.17
31.	Dibutyl ether	130.23
32.	Quinoline	129.16
33.	Isoquinoline	129.16
34.	Phenylbenzene	154.21
Q	Tribromo methane	252.75
36.	Iodo methane	141.94
37.	Ethanethiol	62.13
38.	Propanone	58.08
39.	Butane	58.13
40.	Dipropyl ether	102.18
41.	Fluoro methane	34.03
42.	1,1-dichloro ethane	98.96
43.	1,1-difluroethane	66.05
44.	2-propanol	60.11
45.	1-nitropropane	89.09
46.	2-chloropropane	78.54
47.	Aniline	93.13
48.	Butanal	72.12
49.	m-dichloro-benzene	147.01
50.	m-fluoro-toulene	110.13
51.	Ethane	30.07
52.	Propadiene	40.07
53.	Propene	42.08
54.	Acetylene	26.04
55.	2-chloro-ethanol	80.52
56.	1,3 chclohexadiene	80.14
57.	1-Hexyne	82.15
58.	1,4-dichloro-butane	127.03
59.	Ethanoic acid	60.05
60.	1,3-dichloro propane	112.99
61.	2-chloro-2-methyl propane	92.57
62.	m-chloro-nitro benzene	157.56
63.	p-chloro-nitro benzene	157.56
64.	1,3-cyclopentadiene	66.10
65.	1,3-butadiene	54.09
66.	4-chloro-phenol	128.56
67	1,3-cyclohexadiene	80.14
68.	Phenyl-methanol	108.15
69.	Acetophenone	120.16
70.	p-fluoro-nitrobenzene	141.10